

The Impact of a Bulge on Haemodynamics in an Elastic Compliant Artery

VISHAKHA JADAUN¹

¹Malla Reddy University

September 5, 2022

Abstract

The arterial vascular system exchanges blood gases using pulmonary capabilities. In humans, hemodynamic flows are subjected to periodic velocity modulations. Fluid mechanics and transport of blood gases play an important role in understanding how constitutive relations of the arterial system contribute to human functioning within physiological limits. Assuming the hemodynamic system as a finite dissipative system, the nonlinear evolution equation is perused to understand dynamical challenges under physiological conditions. The infinitesimal component of the vessel wall with concentric thickening in tunica media is considered as a nonaxisymmetric bulge in an elastic-compliant artery. Using the Lie group of transformations method, we discuss the implications of traveling wave solutions to describe their impact on hemodynamic flow in an elastic-compliant artery. We find that cumulative accretion of potential energy contributes to the creation of bright soliton at the apex of the bulge. The wave speed is maximum at the peak of the bulge and progressively retards with the antegrade flow.

Hosted file

KPB_BIO - 030922.tex available at <https://authorea.com/users/443649/articles/584747-the-impact-of-a-bulge-on-haemodynamics-in-an-elastic-compliant-artery>

THE IMPACT OF A BULGE ON HAEMODYNAMICS IN AN ELASTIC COMPLIANT ARTERY

VISHAKHA JADAUN

ABSTRACT. The arterial vascular system exchanges blood gases using pulmonary capabilities. In humans, hemodynamic flows are subjected to periodic velocity modulations. Fluid mechanics and transport of blood gases play an important role in understanding how constitutive relations of arterial system contribute to human functioning within physiological limits. Assuming hemodynamic system as finite dissipative system, the nonlinear evolution equation is perused to understand dynamical challenges under physiological conditions. The infinitesimal component of the vessel wall with concentric thickening in tunica media is considered as a nonaxisymmetric bulge in an elastic-compliant artery. Using Lie group of transformations method, we discuss the implications of traveling wave solutions to describe its impact on hemodynamic flow in an elastic-compliant artery. We find that cumulative accretion of potential energy contributes to creation of bright soliton at the apex of bulge. The wave-speed is maximum at the peak of the bulge and progressively retards with antegrade flow.

1. INTRODUCTION

Pulsatile flows are liable to become turbulent especially cardiovascular flows wherein the largest blood vessels are in the transition scheme *i.e.* increasing and decreasing velocity gradients impact blood flow through entire vascular system. Hemodynamic instabilities and consequent fluid structure alterations are associated with cardiovascular diseases [1–3]. Human physiological flow characteristics such as elasticity, non-Newtonian behavior and complex three-dimensional geometry add difficulties to assess pulsatile flows and transition from laminar to turbulent flow. Even simple scenario of transition in pulsatile Newtonian flows is not adequately understood.

In hemodynamic flow distribution network such as cardiovascular system, the dimensionless numbers help to understand biofluid mechanics because hemodynamic flow determined by a delicate balance between pressure gradient and various stress through biological scaling in vascular network. The velocity fluctuations of human blood flow are implicated in intravascular hemolysis, megakaryocyte activation/amplification, thrombin release/thrombus formation, arteriosclerosis, and atherosclerosis [4, 5]. Noninvasive techniques to measure blood flow include phase-contrast magnetic resonance imaging. Many errors including eddy current, nonlinear gradient, concomitant gradient, or measurement errors get incorporated into velocity gradient. Moreover, turbulent patterns introduce signal losses and artifacts which subsequently limit quality of measurements [6]. Thus, assessing turbulence noninvasively *in vivo* is challenging.

The dimensionless numbers of Womersley, Strouhal and Reynolds have been used to assess transition from laminar to turbulent flow [7]. Earlier Reynolds number was used in hydrodynamics to assess flows in rigid pipe. It was enunciated to study pulsatile flows in elastic compliant arteries, yet it is used to predict different fluid flow situation in biological rheology. The increasing and decreasing velocity gradients during cardiac cycle are postulated to cause turbulence. On one hand, steady flows in rigid pipe under transition scenario [8–11] reveal reduced threshold for turbulence with pulse frequency. On the other hand, studies related to pulsatile flows in straight rigid pipes have contrary findings. It is found that flows can be either linearly stable or linearly unstable [12]. For the onset of turbulence trends, the transition thresholds exhibit opposing trends. [13, 14] suggest that transition threshold increases with increment in unsteady forces over viscous forces, while [15, 16] found that transition threshold decreased when pulse amplitude increased. The transition of pulsatile biological flows is not well understood.

Key words and phrases. Lie symmetry analysis; Solitons solutions; Nonlinear evolution equation; Nonaxisymmetric lesion; Phase parameter; Small-but-finite amplitude wave .

Large elastic arteries deliver oxygenated blood to tissues and buffer pulsatile flows. The shock absorbing capability of large arteries significantly changes with cellular events through the shear stress. The most significant function of large elastic arteries is to reduce impedance owing to left ventricular ejection fraction. The dynamic resistance to the oscillatory component of the cyclic pulsatile flow is achieved by expansion of arterial lumen during cardiac systole and accumulation of blood in large elastic arteries for run-off during cardiac diastole.

Noninvasively, it is quite difficult to accurately measure blood flow. The accurate measurement of intricate wave forms of hemodynamic flow can not be over emphasized. Thus, it is important to study wave forms in blood flow. Since hemodynamic flow is highly nonlinear, few assumptions are ascribed such that principles of continuum mechanics become applicable. To understand hemodynamic flow in large elastic artery, [17, 18] elaborated few assumptions viz. artery is straight, uniform, elastic tube with undisturbed cross-section area; it has ideal visco-elastic properties; blood is homogeneous, incompressible with constant density; viscosity is neglected (since impact of viscosity is confined to thin boundary layers on the vessel wall); velocity profile in large elastic arteries such as aorta is flat. Aforementioned assumptions are needed as the wavelength of initial deformation is longer than the diameter of elastic compliant artery.

The research related to small amplitude waves in elastic compliant arteries focuses on dispersive characteristics of waves while ignoring associated nonlinear effects. [19] evaluated wave form characteristics in elastic compliant arteries based on parameter such as pressure, age & muscular-activation and found a harmonic wave type of traveling wave solution responsible for underlying dispersion relation. On the other hand, [20] considered nonlinear effects to evaluate adaptive response of compliant arteries. The author used nonlinear terms related to constitutive relations of vessel wall of aorta and kinematical equations of fluid-structure interactions. Using NLEEs, the author explained dissipation and pressure diffusion terms depending upon the order of nonlinearity and found that unsteady hemodynamic flow exists in normal elastic compliant artery. The author also indicated that shock formation distances vary from few millimetres to few centimetres depending upon elastic properties of aorta. [21] assessed pulsatile flow in elastic arteries using Navier-Stokes equations and suggested an appropriate numerical method instead of analytical approach to get insight on nonlinear response of vessel wall to a large deformation. [22] elaborated mathematical modeling of initial lesion of aortic dissection. [23] used characteristic method to assess nonlinear equations for one-dimensional flow and found that outflow pulses from left ventricle including diacrotic wave is generated by reflections. [24] assessed wave propagation and shock formation in viscoelastic fluid and found an exact solution with distortionless propagation for a Mooney-Rivlin material.

In recent literature, researchers have employed asymptotic methods to evaluate small amplitude waves. The Korteweg-de Vries equation and the Burgers' equation are representative equations for dispersive media and dissipative media, respectively. These equations exhibit a delicate balance among nonlinearity (that is responsible for steepening of the waves); dissipation (that is responsible for attenuation of the waves); and combination of nonlinearity & dispersion (that is responsible for broadening of waves). Depending upon characteristics of the system, balance relation between dispersion and nonlinearity results into stable nonlinear traveling wave solutions including solitary waves. Whereas in other circumstances, balance relation among dissipation, nonlinearity and dispersion results into the Korteweg-de Vries-Burgers (KdVB) equation.

Also, the propagation of small and finite amplitude waves in elastic complaint arteries has been evaluated. [25] evaluated propagation of small amplitude waves in elastic compliant arteries. The author considered steady state solution of an NLEE to explore damping & dispersion effects. The author found that when laminar elastic jumps are governed by the KdVB equation, solution is invalid as oscillation duration approaches to infinity. [26] evaluated nonlinear pressure wave propagation while accounting convective motion of the fluid, nonlinear strains and stress-strain relations. The author found a relation between multi-soliton solutions and steepening phenomena. [27–29] elucidated dynamic features of pulsatile hemodynamic flow in large elastic compliant arteries using soliton theory. They found that left ventricular ejection fraction excites formation of soliton that aids to the formation of pulse waveform peaks. The propagation of such pulse as diacrotic wave is governed by the KdV equation. Note that the propagation of small amplitude waves in viscoelastic compliant arteries is governed by KdV equation, Burgers' equation and KdVB equation. Various methods [30–38] such as the inverse scattering transformation, Bäcklund transformation, $(\frac{G'}{G})$ -expansion method, Darboux transformation, Hirota method and Lie group of transformations method have been proposed to solve the NLEEs.

The primary motivation for the present work is to elucidate wave propagation in an elastic artery. The goal is to understand the impact of a nonaxisymmetric lesion on propagation of weak nonlinear waves in an elastic compliant artery. For this purpose, in Section 2, we model an equation for the vessel wall of an elastic compliant artery to assess waveforms of underlying blood flow. In section 3, we undertake Lie symmetry analysis for the generalized (3+1)-dimensional NLEE to evaluate changes in the wave speed in proximity of nonaxisymmetric lesion. In Section 4, we evaluate symmetry groups for generalized (3+1)-dimensional NLEE. In Section 5, symmetry reduction and closed form solutions for the generalized (3+1)-dimensional NLEE has been done. Graphical interpretation and discussion in Section 6 reveals impact of lesion on the wave speed. Finally, in Section 7, we present concluding remarks and future scope.

2. MATHEMATICAL FORMULATION OF VESSEL WALL AND BULGE

2.1. Equation of the Vessel Wall of an Elastic Compliant Artery. The pulsatile blood flow inside an elastic artery lumen can not be observed directly. Instead, radial displacement and concomitant elastic recoil aid to assess waveforms of blood flow. Therefore, we derive the equation of the vessel wall of an elastic compliant artery. Consider the elastic artery as a circularly cylindrical elongated tube with radius R_0 . Assume that the elastic artery is a thin-walled incompressible axially prestretched hyperelastic tube with a localized nonaxisymmetric lesion such as intramural haemotoma. This elastic artery is subjected to initial axial stretch π and a uniform pressure inside an elastic compliant artery $\mathcal{E}_0(\mathfrak{z})$.

The position vector of a given point on the elastic artery is given by

$$\vec{\mathbf{r}}_0 = [\mathbf{r}_0 + \mathfrak{f}(z)]e_{\mathfrak{r}} + ze_z, \quad z = \pi \mathfrak{z}, \quad (2.1)$$

where \mathbf{r}_0 is the deformed radius, e_z & e_r are basis vectors, \mathfrak{z} and z are the axial polar coordinate pre-deformation and post-deformation of the elastic artery, respectively and $\mathfrak{f}(z)$ is a function to describe the geometry of nonlinearly dilated aorta in aortic aneurysm and dissection disorders.

After application of the initial static deformation, we superimpose only a dynamical radial displacement $u(z, t)$ to the initial static deformation, then the position vector $\vec{\mathbf{r}}$ of a given point on the elastic artery is given by

$$\vec{\mathbf{r}} = [\mathbf{r}_0 + \mathfrak{f}(z) + u(z, t)]e_{\mathfrak{r}} + ze_z. \quad (2.2)$$

Note that the axially prestretched artery does not undergo significant deformation after application of initial static deformation. dS_z and dS_{θ} are arc-lengths along meridional and longitudinal curves, respectively given by

$$dS_z = \left[1 + \left(\frac{d\mathfrak{f}}{dz} + \frac{\partial u}{\partial z} \right)^2 \right]^{\frac{1}{2}} dz, \quad dS_{\theta} = [\mathbf{r}_0 + \mathfrak{f} + u]d\theta. \quad (2.3)$$

π_1 and π_2 are stretch ratios in the longitudinal and circumferential directions, respectively. In the final configuration these are presented as

$$\pi_1 = \pi \Upsilon, \quad \pi_2 = \frac{1}{R_0}(\mathbf{r}_0 + \mathfrak{f} + u), \quad (2.4)$$

where $\Upsilon = \left[1 + \left(\mathfrak{f}' + \frac{\partial u}{\partial z} \right)^2 \right]^{\frac{1}{2}}$, $\mathfrak{f}' = \frac{d\mathfrak{f}}{dz}$.

Post application of static deformation, \mathbf{t} and \mathbf{n} are unit tangent vector and unit normal vector, respectively along the deformed meridional curve of elastic compliant artery given by

$$\mathbf{t} = \frac{\left(\mathfrak{f}' + \frac{\partial u}{\partial z} \right) e_{\mathfrak{r}} + e_z}{\Upsilon}, \quad \mathbf{n} = \frac{e_{\mathfrak{r}} - \left(\mathfrak{f}' + \frac{\partial u}{\partial z} \right) e_z}{\Upsilon}. \quad (2.5)$$

The longitudinal displacement of elastic compliant artery is relatively small because strong vascular tethering as well as helical circumferential orientation of the elastin and collagen fibers prevents extra ordinary motion. Accordingly assumption of material incompressibility is made about the aortic vessel wall, given by

$$\delta = \frac{\Delta}{\pi_1 \pi_2}, \quad (2.6)$$

where Δ and δ are pre-deformation and post-deformation vessel wall thickness, receptively. The force that acts on the infinitesimal aortic wall component placed between the planes $z = A_1$, $z + dz = A_2$, $\theta = A_3$ and $\theta + d\theta = A_4$, where A_i , $i = 1, \dots, 4$ are arbitrary constants.

The material incompressibility assumption determines the longitudinal displacement of the vessel wall, given by

$$\mathbf{F} = -T_2\Upsilon \left\{ \frac{(\mathbf{r}_0 + \mathbf{f} + u) \left(\mathbf{f}' + \frac{\partial u}{\partial z} \right) T_1}{\Upsilon} \right\} + \mathcal{E}(\mathbf{r}_0 + \mathbf{f} + u)\Upsilon, \quad (2.7)$$

where \mathcal{E} is the fluid reaction force.

T_1 and T_2 are tensions in the longitudinal and circumferential directions given by

$$T_1 = \frac{\mu\Delta}{\pi_2} \frac{\partial\Psi}{\partial\pi_1}, \quad T_2 = \frac{\mu\Delta}{\pi_1} \frac{\partial\Psi}{\partial\pi_2}, \quad (2.8)$$

where μ and Ψ are material shear modulus and strain energy density function of the wall material, respectively.

Finally, the equation of the radial motion of infinitesimal segment of vessel wall of the aorta is given by

$$\frac{\mu}{\pi} \frac{\partial\Psi}{\partial\pi_2} + \mu R_0 \frac{\partial}{\partial z} \left\{ \frac{\left(\mathbf{f}' + \frac{\partial u}{\partial z} \right) \partial\Psi}{\Upsilon} \frac{\partial\Psi}{\partial\pi_1} \right\} + \frac{\mathcal{E}}{\Delta} (\mathbf{r}_0 + \mathbf{f} + u)\Upsilon = \rho \frac{R_0}{\pi} \frac{\partial^2 u}{\partial t^2}, \quad (2.9)$$

where ρ is the mass density of the tube material.

Above equation models aorta as an elastic artery that is an axially prestretched hyperelastic tube. Note that the elastic properties of the injured wall differs from the healthy part. We assume that the constitutive relations of the wall are homogeneous. Thus, material shear modulus μ is constant. Now the above equation holds equivalently valid for normal constitutive features of aorta. Further, we seek to assess the impact of mean blood pressure as pressure reaction force on vessel wall of aorta including the tunica media. In the next subsection, we formulate a boundary value problem in this regard.

2.2. Equation of the Bulge, Nonaxisymmetric Lesion in the Vessel Wall. The propagation of pulsatile blood flow in an elastic artery is impacted by arterial mechanics. It means that small but finite amplitude waves undergo drastic transformations due to nonlinearity introduced by nonaxisymmetric lesion in the vessel wall of elastic compliant artery. Assume that the elastic compliant artery is a thin walled incompressible axially prestretched hyperelastic tube with localized nonaxisymmetric lesion. Note that such lesions are found in atypical aortic aneurysm and dissection disorders including intramural haemotoma.

To formulate the equation for the nonaxisymmetric lesion, we consider an infinitesimal component of the vessel wall of an elastic compliant artery, wherein concentric thickening of tunica media creates a bulge into tunica intima. Since the bulge ($l(t)$) is hyperbolic secant type, it is mathematically expressed as

$$l(t) = c \operatorname{sech}^2(Kt). \quad (2.10)$$

Note that $l(t)$ characterizes the bulge, K and c are constants, where c is positive.

From clinical perspective, order parameters emerge from symmetry-breaking. Such symmetry-breaking transitions occur across boundaries in a phase transition system. At a particular critical point, the order parameter susceptibility usually diverge. To say, wave propagation in an elastic compliant artery is a homeostatic process. With emergence of bulge, the symmetry of wave propagation is broken and the next critical point is not same. Thus, phase parameter characterizes continuous phase transitions, wherein wave speed is affected by the bulge. The equation of phase parameter ϑ has the following form

$$\vartheta = \sqrt{\frac{a_0}{12}} \exp\left(\frac{-2t}{3}\right) \left\{ \theta - \frac{a_0}{4} \left[1 - \exp\left(\frac{-4t}{3}\right) \right] + \frac{c}{K} \tanh(Kt) \right\}, \quad (2.11)$$

where t is a space variable, a_0 is a constant characterizing the amplitude of the traveling wave at the center of the bulge. The wave speed is defined as

$$v = \frac{1}{\beta - c \operatorname{sech}^2(Kt)}, \quad \beta = \frac{a_0}{3} \exp\left(\frac{-4t}{3}\right), \quad (2.12)$$

where $\frac{1}{\beta}$ is wave speed when cross sectional diameter is constant along the tube axis.

3. METHOD OF LIE GROUP SYMMETRIES FOR (3 + 1)-DIMENSIONAL NLEE

The prevalence and the catastrophic complications of intramural haematoma motivates us to study the impact of presence of axially asymmetric hump like lesion with convex projection in the lumen of an elastic compliant artery, where it interact with pulsatile blood flow. We model and analyze the (3+1)-dimensional nonlinear evolution equation with perturbation term, dissipation term and pressure term including linear and nonlinear terms.

In the current work, we aim to study (3+1)-dimensional Kadomstev-Petviashvili-Boussinesq equation, given as

$$\Delta := w_{rrrs} + 3w_r w_{rs} + 3w_s w_{rr} + w_{tt} + w_{rt} + w_{st} - w_{qq} = 0. \quad (*)$$

It is to be noted that KdV equation and the KP equation are integrable nonlinear evolution equations represented by a first-order partial differential equation (PDE) in time, while Kadomstev-Petviashvili-Boussinesq equation is represented by second-order nonlinear PDE in time. Moreover, it models both (right and left)-going waves.

Using Lie symmetry analysis similarity reductions of the NLEE is derived as given in [36, 37]. Consider the one parameter Lie group of infinitesimal transformation

$$\begin{aligned} \dot{r} &= r + \varsigma \xi^1(r, s, q, t, w) + O(\varsigma^2) \\ \dot{s} &= s + \varsigma \xi^2(r, s, q, t, w) + O(\varsigma^2) \\ \dot{q} &= q + \varsigma \xi^3(r, s, q, t, w) + O(\varsigma^2) \\ \dot{t} &= t + \varsigma \tau(r, s, q, t, w) + O(\varsigma^2) \\ \dot{w} &= w + \varsigma \eta(r, s, q, t, w) + O(\varsigma^2), \end{aligned} \quad (3.1)$$

where ς is group parameter and ξ^1 , ξ^2 , ξ^3 , τ are the generators of Lie group transformations for independent variables while η for dependent variable. The associated vector field is represented by

$$X = \xi^1(r, s, q, t, w) \partial_x + \xi^2(r, s, q, t, w) \partial_y + \xi^3(r, s, q, t, w) \partial_z + \tau(r, s, q, t, w) \partial_t + \eta(r, s, q, t, w) \partial_w.$$

The infinitesimal criteria for the invariance of the Eq. (*) is

$$\eta_{rrrs} + 3\eta_r w_{rs} + 3w_r \eta_{rs} + 3\eta_s w_{rr} + 3\eta_{rr} w_s + \eta_{tt} + \eta_{rt} + \eta_{st} - \eta_{qq} = 0. \quad (3.2)$$

It is obtained from the invariance condition, $Pr^{(4)}X(\Delta) = 0$ whenever $\Delta = 0$. Applying the fourth prolongation $Pr^{(4)}X$ of X to Eq. (3.2), we obtain determining equations which are constituted of overdetermined system of coupled partial differential equations

$$\begin{aligned} \xi_t^1 &= \xi_r^1 = \frac{\xi_q^3}{3}, \quad \xi_w^1 = 0, \quad \xi_s^1 = 0, \quad \xi_q^1 = \frac{\xi_t^3}{2} = 0 \\ \xi_t^2 &= \xi_q^2 = \xi_w^2 = 0, \quad \xi_s^2 = \xi_q^3, \quad \xi_q^2 = \frac{\xi_t^3}{2} \\ \xi_w^3 &= \xi_r^3 = \xi_s^3 = \xi_{tt}^3 = \xi_{tq}^3 = \xi_{qq}^3 = 0 \\ \tau_t &= \xi_q^3, \quad \tau_r = \tau_w = \tau_s = 0, \quad \tau_q = \xi_t^3 \\ \eta_w &= -\frac{\xi_q^3}{3}, \quad \eta_r = \frac{\xi_q^3}{9} = \eta_s, \quad \eta_{tt} = \eta_{qq}. \end{aligned} \quad (3.3)$$

Solving determining Eqs. (3.3) yield infinitesimal generators

$$\begin{aligned}
\xi^1 &= \frac{c_1}{2}q + \frac{c_2}{3}(r+t) + c_6 \\
\xi^2 &= 2c_4s + \frac{a}{c}c_3t + c_6 \\
\xi^3 &= \frac{c_1}{2}q + c_2s + c_3 \\
\tau &= c_1t + c_2q + c_3 \\
\eta &= \varphi(t-q) + \psi(t+q) + \frac{c_2}{9}(r+s-3w)
\end{aligned} \tag{3.4}$$

where $c_i, i = 1, \dots, 6$ and $\varphi(t-q)$ & $\psi(t+q)$ are arbitrary constants and arbitrary functions, respectively. Assume $\varphi(t-z) = c_7$, following vector fields span the Lie algebra of infinitesimal symmetries of the Eq. (*)

$$\begin{aligned}
X_1 &= \frac{q}{2}\frac{\partial}{\partial r} + \frac{q}{2}\frac{\partial}{\partial s} + t\frac{\partial}{\partial r} + q\frac{\partial}{\partial t} \\
X_2 &= \frac{(r+t)}{3}\frac{\partial}{\partial r} + s\frac{\partial}{\partial s} + q\frac{\partial}{\partial r} + t\frac{\partial}{\partial t} + \frac{(r+s-3w)}{9}\frac{\partial}{\partial w} \\
X_3 &= \frac{\partial}{\partial q}, \quad X_4 = \frac{\partial}{\partial t}, \quad X_5 = \frac{\partial}{\partial s}, \quad X_6 = \frac{\partial}{\partial r}, \quad X_7 = \frac{\partial}{\partial w}.
\end{aligned} \tag{3.5}$$

It is simple to exhibit the commutation relation of a Lie algebra through its Lie bracket table having $(i, j)^{th}$ entry is $[X_i, X_j] = X_i * X_j = X_i \cdot X_j - X_j \cdot X_i$. The commutator table is skew-symmetric since $[X_\alpha, X_\beta] = -[X_\beta, X_\alpha]$. Given commutator table is formed for the vector fields (3.5)

TABLE 1. Commutator table of Lie algebra

*	X_1	X_2	X_3	X_4	X_5	X_6	X_7
X_1	0	0	$\frac{X_5 - X_6}{2} + X_4$	$-X_3$	0	0	0
X_2	0	0	$-X_3$	$-\frac{X_6}{3} - X_4$	$-X_5 - \frac{X_7}{9}$	$-\frac{X_6}{3} - \frac{X_7}{9}$	$\frac{X_7}{3}$
X_3	$-\frac{X_5 + X_6}{2} - X_4$	X_3	0	0	0	0	0
X_4	X_3	$\frac{X_6}{3} + X_4$	0	0	0	0	0
X_5	0	$X_5 + \frac{X_7}{9}$	0	0	0	0	0
X_6	0	$\frac{X_6}{3} + \frac{X_7}{9}$	0	0	0	0	0
X_7	0	$-\frac{X_7}{3}$	0	0	0	0	0

As reflected in the table above, the generalized (3+1)-dimensional NLEE contains a continuous group of transformations which is generated by the infinite-dimensional Lie algebra spanned by vector fields (3.5). Since the infinite number of subalgebras for this Lie algebra are constituted from linear combinations of generators, in our case $X_i, i = 1, 2, \dots, 7$.

4. SYMMETRY GROUPS FOR (3 + 1)-DIMENSIONAL NLEE

Using vector fields X_i for $i = 1, 2, \dots, 7$, we obtain the group transformations, $\mathbf{G}_i : (r, s, q, t, w) \rightarrow (\check{r}, \check{s}, \check{q}, \check{t}, \check{w})$, and solve the following system of ordinary differential equations (ODEs)

$$\begin{aligned}
\frac{d(\check{r}, \check{s}, \check{q}, \check{t}, \check{w})}{d\zeta} &= (\xi^1, \xi^2, \xi^3, \tau, \eta), \\
(\check{r}, \check{s}, \check{q}, \check{t}, \check{w})|_{\zeta=0} &= (r, s, q, t, w).
\end{aligned}$$

The one parameter groups \mathbf{G}_i spanned by X_i are given by

$$\begin{aligned}
\mathbf{G}_1 : (r, s, q, t, w) &\rightarrow \left(r + \varsigma \frac{q}{2}, s + \varsigma \frac{q}{2}, q + \varsigma t, t + \varsigma q, w \right) \\
\mathbf{G}_2 : (r, s, q, t, w) &\rightarrow \left(r + \varsigma \frac{r+t}{3}, s + \varsigma s, q + \varsigma q, t + \varsigma t, w + \varsigma \frac{r+s-3w}{9} \right) \\
\mathbf{G}_3 : (r, s, q, t, w) &\rightarrow (r, s, q + \varsigma, t, w) \\
\mathbf{G}_4 : (r, s, q, t, w) &\rightarrow (r, s, q, t + \varsigma, w) \\
\mathbf{G}_5 : (r, s, q, t, w) &\rightarrow (r, s + \varsigma, q, t, w) \\
\mathbf{G}_6 : (r, s, q, t, w) &\rightarrow (r + \varsigma, s, q, t, w) \\
\mathbf{G}_7 : (r, s, q, t, w) &\rightarrow (r, s, q, t, w + \varsigma).
\end{aligned} \tag{4.1}$$

The resultant transformed points, $\exp(r, s, q, t, w) = (\overset{\circ}{r}, \overset{\circ}{s}, \overset{\circ}{q}, \overset{\circ}{t}, \overset{\circ}{w})$, generated by above groups $\mathbf{G}_i (i = 1, 2, \dots, 7)$ yield invariant solutions $w_i (i = 1, 2, \dots, 7)$ of Eq. (*) as follows

$$\begin{aligned}
w_1 &= f \left(r - \varsigma \frac{q}{2}, s - \varsigma \frac{q}{2}, q - \varsigma, t - \varsigma \right) \\
w_2 &= \frac{r+s}{3} - \frac{1}{3} f \left(\frac{3r-t}{\varsigma}, \frac{s}{1+\varsigma}, \frac{q}{1+\varsigma}, \frac{t}{1+\varsigma} \right) \\
w_3 &= f(r, s - \varsigma, q, t) \\
w_5 &= f(r, s - \varsigma, q, t) \\
w_6 &= f(r - \varsigma, s, q, t) \\
w_7 &= -\varsigma + f(r, s, q, t).
\end{aligned} \tag{4.2}$$

5. SYMMETRY REDUCTION AND GRAPHICAL REPRESENTATION OF SOLUTIONS

In this section, we perused reduction equations for group invariant solutions for Eq. (*). Since invariant functions are the constant of integration of the characteristic equations, we solve Lagrange's system of characteristic equations given by

$$\frac{dr}{\xi^1(r, s, q, t, w)} = \frac{ds}{\xi^2(r, s, q, t, w)} = \frac{dq}{\xi^3(r, s, q, t, w)} = \frac{dt}{\tau(r, s, q, t, w)} = \frac{dw}{\eta(r, s, q, t, w)}. \tag{5.1}$$

Invariance is remarkable property of Lie group of transformations method. The solutions obtained under one parameter Lie group of transformations are invariant. The Lagrange system of characteristic equations allows group invariant solution to construct differential equation with one-less independent variable, resulting into a ordinary differential equation (ODE). The solution of ODE is back substituted to yield solution of primary differential equation.

5.1. Vector field \mathbf{X}_1 .

$$X_1 = \frac{q}{2} \frac{\partial}{\partial r} + \frac{q}{2} \frac{\partial}{\partial s} + t \frac{\partial}{\partial r} + q \frac{\partial}{\partial t}. \tag{5.2}$$

The Eqs. (5.2) and (5.1) are being used to find associated Lagrange's system

$$\frac{dr}{\frac{q}{2}} = \frac{ds}{\frac{q}{2}} = \frac{dq}{t} = \frac{dt}{q} = \frac{dw}{0}.$$

The invariant functions and invariant solution for the Eq. (*) are

$$w(r, s, q, t) = f(R, S, Q), \quad \text{where } R = 2r - t, \quad S = 2s - t \quad \text{and} \quad Q = q^2 - t^2. \tag{5.3}$$

From Eqs. (5.3) and (*), we get following PDE

$$-f_Q - 4Qf_{QQ} - f_{SS} - 2f_{RS} - f_{RR} + 24f_Rf_{RS} + 24f_Sf_{RR} + 16f_{RRRS} = 0. \quad (5.4)$$

Using similarity transformation method (STM), the new set of infinitesimal generators for Eq. (5.4) is

$$\begin{aligned} \xi_R &= \frac{a_1}{4}R + a_3 \\ \xi_S &= \frac{a_1}{2}S + a_2 \\ \xi_Q &= a_1Q \\ \eta_f &= a_5 \log Q + \frac{a_1}{48}(R + S) + a_4, \end{aligned} \quad (5.5)$$

where ξ_R , ξ_S , ξ_Q are the generators of infinitesimal transformations for independent variables R , S , Q , respectively while η_f for dependent variable f ; a_i , $i = 1, \dots, 5$ are arbitrary constants.

A set of vector fields for generators of infinitesimal transformation (5.5) is given by

$$\begin{aligned} \pi_1 &= \frac{R}{4} \frac{\partial}{\partial R} + \frac{S}{2} \frac{\partial}{\partial S} + Q \frac{\partial}{\partial Q} + \frac{R+S}{48} \frac{\partial}{\partial f}, \\ \pi_2 &= \frac{\partial}{\partial S}, \quad \pi_3 = \frac{\partial}{\partial R}, \quad \pi_4 = \frac{\partial}{\partial f}, \quad \pi_5 = \log Q \frac{\partial}{\partial f}. \end{aligned} \quad (5.6)$$

5.1.1. *Vector field π_2 .*

$$\pi_2 = \frac{\partial}{\partial S}.$$

Lagrange's characteristic for vector field π_2 are

$$\frac{dR}{0} = \frac{dS}{1} = \frac{dQ}{0} = \frac{df}{0}.$$

Further, we write the function f in following similarity form

$$f(R, S, Q) = H(x, y) \quad \text{and} \quad x = R, \quad y = Q, \quad (5.7)$$

where x and y are similarity variables. We reduce Eq. (5.4) into following PDE

$$H_y + 4H_{yy} + H_{xx} = 0. \quad (5.8)$$

Using back substitution, the solution of the Eq. (5.8) provides the solution of primary equation (*) given by

$$w(r, s, q, t) = \frac{(q^2 - t^2)^{\frac{3}{8}} (C_1^2 \exp(C_1(2r - t)^2) + C_2) \left[\text{BesselJ}\left(\frac{3}{4}, \sqrt{-C_1(q^2 - t^2)}\right)C_3 + \text{BesselY}\left(\frac{3}{4}, \sqrt{-C_1(q^2 - t^2)}\right)C_4 \right]}{\exp(\sqrt{C_1}(2r - t))}, \quad (5.9)$$

where C_i , $i = 1, \dots, 4$ are arbitrary constants.

5.1.2. *Vector field π_3 .* Lagrange's characteristic equations for vector field π_3 are

$$\frac{dR}{1} = \frac{dS}{0} = \frac{dQ}{0} = \frac{df}{0}.$$

Further, we write the function f in following similarity form

$$f(R, S, Q) = H(x, y) \quad \text{and} \quad x = S, \quad y = Q, \quad (5.10)$$

where x and y are similarity variables. We reduce Eq. (5.4) into following PDE

$$H_y + 4H_{yy} + H_{xx} = 0. \quad (5.11)$$

Using back substitution, the solution of the Eq. (5.11) provide solution of primary Eq. (*) is

$$w(r, s, q, t) = \frac{(q^2 - t^2)^{\frac{3}{8}} (C_1^2 \exp(C_1(2s - t)^2) + C_2) \left[\text{BesselJ}\left(\frac{3}{4}, \sqrt{-C_1(q^2 - t^2)}\right)C_3 + \text{BesselY}\left(\frac{3}{4}, \sqrt{-C_1(q^2 - t^2)}\right)C_4 \right]}{\exp(\sqrt{C_1}(2s - t))}, \quad (5.12)$$

where $C_i, i = 1, \dots, 4$ are arbitrary constants.

5.2. Vector field X_3 .

$$X_3 = \frac{\partial}{\partial q}.$$

The corresponding Lagrange's characteristic equations is found using Eq. (5.1)

$$\frac{dr}{0} = \frac{ds}{0} = \frac{dq}{1} = \frac{dt}{0} = \frac{dw}{0}. \quad (5.13)$$

The similarity reduction of Eq. (*) is

$$w(r, s, q, t) = f(R, S, T), \quad \text{and} \quad R = r, \quad S = s, \quad T = t, \quad (5.14)$$

where R, S and T are invariant variables.

From the Eqs. (5.14) and (*), we get following PDE

$$f_{RRRS} + 3f_R f_{RY} + 3f_S f_{RR} + f_{RT} + f_{ST} + f_{TT} = 0. \quad (5.15)$$

We find traveling wave solution of Eq. (5.15) are

$$f(R, S, T) = 2C_2 \tanh \left(C_2 R + C_3 S + \left(-\frac{C_2 + C_3}{2} - \frac{1}{2} \sqrt{-16C_2^3 C_3 + C_2^2 + 2C_2 C_3 + C_3^2} \right) T + C_1 \right) + C_5, \quad (5.16)$$

$$f(R, S, T) = 2C_2 \tanh \left(C_2 R + C_3 S + \left(-\frac{C_2 + C_3}{2} + \frac{1}{2} \sqrt{-16C_2^3 C_3 + C_2^2 + 2C_2 C_3 + C_3^2} \right) T + C_1 \right) + C_5. \quad (5.17)$$

Now, we obtain following traveling wave solutions of Eq. (*)

$$w(r, s, q, t) = 2C_2 \tanh \left(C_2 r + C_3 s + \left(-\frac{C_2 + C_3}{2} - \frac{1}{2} \sqrt{-16C_2^3 C_3 + C_2^2 + 2C_2 C_3 + C_3^2} \right) t + C_1 \right) + C_5, \quad (5.18)$$

$$w(r, s, q, t) = 2C_2 \tanh \left(C_2 r + C_3 s + \left(-\frac{C_2 + C_3}{2} + \frac{1}{2} \sqrt{-16C_2^3 C_3 + C_2^2 + 2C_2 C_3 + C_3^2} \right) t + C_1 \right) + C_5, \quad (5.19)$$

where $C_i, i = 1, \dots, 5$ are arbitrary constants.

To obtain variety of the solutions, now we use Lie group of transformations method to obtain a set of infinitesimal generator for Eq. (5.15)

$$\begin{aligned} \xi_R &= \frac{a_1}{3}(R + T) + a_4, \\ \xi_S &= a_1 S + a_3, \\ \tau_T &= a_1 T + a_2, \\ \eta_f &= \frac{a_1}{9}(R + S - 3f) + a_5 T + a_6, \end{aligned}$$

where $a_i, i = 1, \dots, 6$ are arbitrary constants.

Vector fields associated to aforementioned infinitesimal generators are given by

$$\begin{aligned}\pi_1 &= \frac{R+T}{3} \frac{\partial}{\partial R} + S \frac{\partial}{\partial S} + T \frac{\partial}{\partial T} + \frac{R+S-3f}{9} \frac{\partial}{\partial f}, \\ \pi_2 &= \frac{\partial}{\partial T}, \quad \pi_3 = \frac{\partial}{\partial S}, \quad \pi_4 = \frac{\partial}{\partial R}, \quad \pi_5 = T \frac{\partial}{\partial f}, \quad \pi_6 = \frac{\partial}{\partial f}.\end{aligned}\tag{5.20}$$

5.2.1. *Vector field π_2 .*

$$\pi_2 = \frac{\partial}{\partial T}.$$

The Lagrange's characteristic equations for Eq. (5.15) are given by

$$\frac{dR}{0} = \frac{dS}{0} = \frac{dT}{1} = \frac{df}{0}.$$

By solving these equations, we write f in the terms of $H(x, y)$, an invariant function

$$f(R, S, T) = H(x, y), \quad \text{where } x = R \quad \text{and} \quad y = S \quad \text{are similarity variables.}\tag{5.21}$$

Further, the Eq. (5.15) is reduced into following PDE

$$3H_x H_{xy} + 3H_y H_{xx} + H_{xxx} = 0.\tag{5.22}$$

Apply Lie group of transformations method on Eq. (5.22) to obtain infinitesimal generators

$$\begin{aligned}\xi_x &= b_1 x + b_2, \\ \xi_y &= P(y), \\ \eta_H &= -b_1 H + b_3,\end{aligned}$$

where b_1 and b_2 are arbitrary constants.

Assuming $P(y) = 0$, the invariant solution $H(x, y)$ is written as

$$H(x, y) = \frac{G(\zeta)}{x + b_2} \quad \text{with invariant variable } \zeta = y.\tag{5.23}$$

Using above invariant function, Eq. (5.22) is reduced into following ODE

$$6G(\zeta)G'(\zeta) - 6G'(\zeta) + 3G'^2(\zeta) = 0.\tag{5.24}$$

We back substitute the solutions of Eq. (5.24) to obtain solutions of Eq. (*)

$$w(r, s, q, t) = \frac{1 + C_1 \exp(-2s)}{r + C_2} + C_3,\tag{5.25}$$

$$w(r, s, q, t) = \frac{C_1}{r + C_2} + C_3,\tag{5.26}$$

where C_1, C_2 and C_3 are arbitrary constants.

5.2.2. *Vector field* π_3 .

$$\pi_3 = \frac{\partial}{\partial S}.$$

Lagrange's characteristic equations for vector field π_3 are

$$\frac{dR}{0} = \frac{dS}{1} = \frac{dT}{0} = \frac{df}{0}.$$

By solving these equations, we write f in the terms of $H(x, y)$, an invariant function

$$f(R, S, T) = H(x, y), \quad \text{where } x = R \quad \text{and} \quad y = T \quad \text{are similarity variables.} \quad (5.27)$$

Further, the Eq. (5.15) is reduced into following PDE

$$H_{yy} + H_{xy} = 0. \quad (5.28)$$

The solutions of Eq. (*) are

$$w(r, s, q, t) = C_7 \tanh^3(C_3(t - r) - C_1) + C_5 \tanh(C_3(t - r) - C_1) + C_4, \quad (5.29)$$

$$w(r, s, q, t) = C_7 \tanh^3(C_3(t - r) - C_1) + C_6 \tanh^2(C_3(t - r) - C_1) + C_5 \tanh(C_3(t - r) - C_1) + C_4, \quad (5.30)$$

where $C_i, i = 1, \dots, 7$ are arbitrary constants.

5.2.3. *Vector field* π_4 .

$$\pi_4 = \frac{\partial}{\partial R}.$$

Lagrange's characteristic equations are calculated as follows

$$\frac{dR}{1} = \frac{dS}{0} = \frac{dT}{0} = \frac{df}{0}.$$

By solving these equations, we write the function f in the terms of invariant function $H(x, y)$

$$f(R, S, T) = H(x, y), \quad \text{where } x = S \quad \text{and} \quad y = T \quad \text{are similarity variables.} \quad (5.31)$$

Using above invariant function, the reduced PDE from the Eq. (5.15) is

$$H_{yy} + H_{xy} = 0. \quad (5.32)$$

The solutions of Eq. (*) are

$$w(r, s, q, t) = C_7 \tanh^3(C_3(t - s) - C_1) + C_5 \tanh(C_3(t - s) - C_1) + C_4, \quad (5.33)$$

$$w(r, s, q, t) = C_7 \tanh^3(C_3(t - s) - C_1) + C_6 \tanh^2(C_3(t - s) - C_1) + C_5 \tanh(C_3(t - s) - C_1) + C_4. \quad (5.34)$$

5.3. **Vector field** \mathbf{X}_4 .

$$\mathbf{X}_4 = \frac{\partial}{\partial t}.$$

The associated Lagrange's characteristic equations are as follows,

$$\frac{dr}{0} = \frac{ds}{0} = \frac{dq}{0} = \frac{dt}{1} = \frac{dw}{0}.$$

The Eq. (*) is written in the form of invariant function $f(R, S, Q)$

$$w(r, s, q, t) = f(R, S, Q), \quad \text{where } R = r, \quad S = s \quad \text{and} \quad Q = q. \quad (5.35)$$

From Eqs. (5.35) and (*), the primary equation with one-less independent variable is written as

$$3f_R f_{RS} + 3f_Y f_{RR} + f_{RRRS} - f_{QQ} = 0. \quad (5.36)$$

The traveling wave solutions of Eq. (5.36) are

$$f(R, S, Q) = 2C_2 \tanh(C_2 R + C_3 S - 2\sqrt{C_2^3 C_3} Q + C_1) + C_5, \quad (5.37)$$

$$f(R, S, Q) = 2C_2 \tanh(C_2 R + C_3 S + 2\sqrt{C_2^3 C_3} Q + C_1) + C_5. \quad (5.38)$$

$$(5.39)$$

Therefore, solutions of main Eq. (*) can be written as

$$w(r, s, q, t) = 2C_2 \tanh(C_2 r + C_3 s - 2\sqrt{C_2^3 C_3} q + C_1) + C_5, \quad (5.40)$$

$$w(r, s, q, t) = 2C_2 \tanh(C_2 r + C_3 s + 2\sqrt{C_2^3 C_3} q + C_1) + C_5. \quad (5.41)$$

$$(5.42)$$

Now the new set of infinitesimal generators for (5.36) by applying similarity transformations method (STM) is

$$\begin{aligned} \xi_R &= \frac{1}{3}(2a_1 - a_3)R + a_5, \\ \xi_S &= a_3 S + a_4, \\ \xi_Q &= a_1 Q + a_2, \\ \eta_f &= -\frac{1}{3}(2a_1 - a_3)f + a_6 Q + a_7, \end{aligned}$$

where ξ_R , ξ_S , ξ_Q and η_f are infinitesimal generators; a_i , $i = 1, \dots, 7$ are arbitrary constants. The vector fields associated to these infinitesimal generators are

$$\begin{aligned} \pi_1 &= \frac{2R}{3} \frac{\partial}{\partial R} + Q \frac{\partial}{\partial Q} - \frac{2f}{3} \frac{\partial}{\partial f}, \\ \pi_2 &= \frac{\partial}{\partial Q}, \quad \pi_3 = -\frac{R}{3} \frac{\partial}{\partial R} + S \frac{\partial}{\partial S} + \frac{f}{3} \frac{\partial}{\partial f}, \\ \pi_4 &= \frac{\partial}{\partial S}, \quad \pi_5 = \frac{\partial}{\partial R}, \quad \pi_6 = Q \frac{\partial}{\partial f}, \quad \pi_7 = \frac{\partial}{\partial f}. \end{aligned} \quad (5.43)$$

5.3.1. *Vector field π_2 .*

$$4\pi_2 = \frac{\partial}{\partial Q}.$$

The similarity reduction of Eq. (5.36) is given by

$$f(R, S, Q) = H(x, y), \quad \text{where } x = R \text{ and } y = S. \quad (5.44)$$

The Eq. (5.36) is reduced in a PDE with two independent variables

$$3H_x H_{xy} + 3H_y H_{xx} + H_{xxx} = 0. \quad (5.45)$$

Lie group analysis method gives the following infinitesimals when it applies on Eq. (5.45).

$$\begin{aligned} \xi_x &= b_1 x + b_2, \\ \xi_y &= P(y), \\ \eta_H &= -b_1 H + b_3, \end{aligned}$$

where b_1 and b_2 are arbitrary constants.

Assuming $P(y) = 0$, the function $H(x, y)$ is written in the form of invariant function $G(\zeta)$

$$H(x, y) = \frac{G(\zeta)}{x + b_2}, \quad \text{where } \zeta = y. \quad (5.46)$$

Using above invariant function, Eq. (5.45) is reduced into a first order ODE

$$6G(\zeta)G'(\zeta) - 6G'(\zeta) + 3G'^2(\zeta) = 0. \quad (5.47)$$

To find solutions of the Eq. (*), we back substitute the solutions of Eq. (5.47)

$$w(r, s, q, t) = \frac{1 + C_1 \exp(-2s)}{r + C_2} + C_3, \quad (5.48)$$

$$w(r, s, q, t) = \frac{C_1}{r + C_2} + C_3, \quad (5.49)$$

where C_1 , C_2 and C_3 are arbitrary constants.

5.3.2. Vector field π_4 .

$$\pi_4 = \frac{\partial}{\partial S}.$$

The vector field π_4 provide similarity reduction of Eq. (5.36) as follows

$$f(R, S, Q) = H(x, y), \quad \text{where } x = R \text{ and } y = Q. \quad (5.50)$$

By using Eq. (5.50), reduction of Eq. (5.36) is

$$H_{yy} = 0. \quad (5.51)$$

Hence, solution of the Eq. (*) in this case is

$$w(r, s, q, t) = \alpha(r)q + \beta(r), \quad (5.52)$$

where $\alpha(r)$ and $\beta(r)$ are arbitrary functions of r .

5.3.3. Vector field π_5 .

$$\pi_4 = \frac{\partial}{\partial R}.$$

The vector field π_4 provide similarity reduction of Eq. (5.36) as follows

$$f(R, S, Q) = H(x, y), \quad \text{where } x = S \text{ and } y = Q \quad (5.53)$$

By using Eq. (5.53), reduction of Eq. (5.36) is

$$H_{yy} = 0. \quad (5.54)$$

Hence, solution of Eq. (*) in this case is

$$w(r, s, q, t) = \alpha(s)q + \beta(s). \quad (5.55)$$

where $\alpha(s)$ and $\beta(s)$ are arbitrary functions of s .

5.4. Vector field X_5 .

$$X_5 = \frac{\partial}{\partial s}. \quad (5.56)$$

Using Eqs. (5.56) and (5.1), we find following Lagrange's characteristic equations

$$\frac{dr}{0} = \frac{ds}{1} = \frac{dq}{0} = \frac{dt}{0} = \frac{dw}{0}$$

The reduce form of Eq. (*) in invariant function $f(S, Q, T)$ is

$$w(r, s, q, t) = f(S, Q, T), \quad \text{where } R = r, \quad Q = q \quad \text{and} \quad T = t. \quad (5.57)$$

From Eqs. (5.57) and (*), following PDE is obtained

$$f_{RT} + f_{TT} - f_{QQ} = 0. \quad (5.58)$$

By solving Eq. (5.58), we obtain following travelling wave solutions of the primary equation (*)

$$w(r, s, q, t) = C_8 \tanh^3 \left(C_3 t - \frac{C_3^2 - C_4^2}{C_3} r + C_4 q + C_1 \right) + C_6 \tanh \left(C_3 t - \frac{C_3^2 - C_4^2}{C_3} r + C_4 q + C_1 \right) + C_5, \quad (5.59)$$

$$\begin{aligned} w(r, s, q, t) &= C_8 \tanh^3 \left(C_3 t - \frac{C_3^2 - C_4^2}{C_3} r + C_4 q + C_1 \right) + C_7 \tanh^2 \left(C_3 t - \frac{C_3^2 - C_4^2}{C_3} r + C_4 q + C_1 \right) \\ &\quad + C_6 \tanh \left(C_3 t - \frac{C_3^2 - C_4^2}{C_3} r + C_4 q + C_1 \right) + C_4, \end{aligned} \quad (5.60)$$

where $C_i, i = 1, \dots, 8$ are arbitrary constants.

5.5. Vector field X_6 .

$$X_6 = \frac{\partial}{\partial r}. \quad (5.61)$$

Using Eqs. (5.61) and (5.1), we find following Lagrange's characteristic equations

$$\frac{dr}{1} = \frac{ds}{0} = \frac{dq}{0} = \frac{dt}{0} = \frac{dw}{0}.$$

The reduced form of Eq. (*) in invariant function $f(S, Q, T)$ is

$$w(r, s, q, t) = f(S, Q, T), \quad \text{where } S = s, \quad Q = q \quad \text{and} \quad T = t. \quad (5.62)$$

From Eqs. (5.62) and (*), following PDE is obtained

$$f_{ST} + f_{TT} - f_{QQ} = 0. \quad (5.63)$$

By solving Eq. (5.63), we obtain following travelling wave solutions of the Eq. (*)

$$w(r, s, q, t) = C_8 \tanh^3 \left(C_3 t - \frac{C_3^2 - C_4^2}{C_3} s + C_4 q + C_1 \right) + C_6 \tanh \left(C_3 t - \frac{C_3^2 - C_4^2}{C_3} s + C_4 q + C_1 \right) + C_5, \quad (5.64)$$

$$\begin{aligned} w(r, s, q, t) &= C_8 \tanh^3 \left(C_3 t - \frac{C_3^2 - C_4^2}{C_3} s + C_4 q + C_1 \right) + C_7 \tanh^2 \left(C_3 t - \frac{C_3^2 - C_4^2}{C_3} s + C_4 q + C_1 \right) \\ &\quad + C_6 \tanh \left(C_3 t - \frac{C_3^2 - C_4^2}{C_3} s + C_4 q + C_1 \right) + C_4, \end{aligned} \quad (5.65)$$

where $C_i, i = 1, \dots, 8$ are arbitrary constants.

6. GRAPHICAL INTERPRETATION AND DISCUSSION

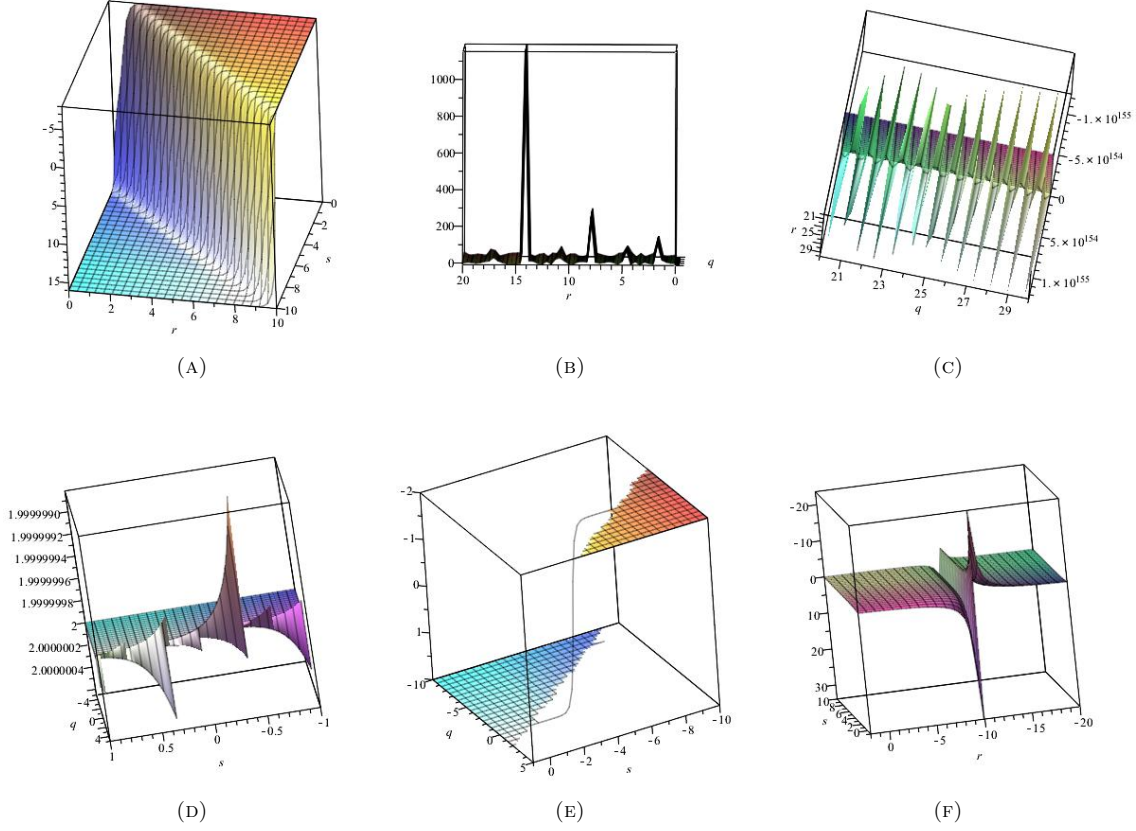


FIGURE 1. (A) In Eq. (5.29), $C_1 = 1, C_3 = 3, C_4 = 4, C_5 = 5, C_7 = 7$ and $-10 \leq r, s \leq 10$, (B) In Eq. (5.55), $\alpha(r) = \sin(r^2)$, $\beta(r) = \sec^2(r)$ and $-10 \leq r, q \leq 10$, (C) In Eq. (5.9), $t = 10.358$, $C_1 = 50$, $C_2 = 2$, $C_3 = 3$, $C_4 = 4$ and $20 \leq r, q \leq 30$, (D) In Eq. (5.18), $r = 1.025$, $C_1 = 11$, $C_2 = 2$, $C_3 = 3$, $C_5 = 1$ and $-1 \leq s \leq 1$, $-5 \leq q \leq 5$, (E) In Eq. (5.18), $r = 0.025$, $C_1 = 11$, $C_2 = 2$, $C_3 = 3$, $C_5 = 1$ and $-10 \leq s \leq 1$, $-10 \leq q \leq 5$, (F) In Eq. (5.25), $C_1 = 1.98$, $C_2 = 10.105$, $C_3 = 1.508$ and $-20 \leq r \leq 2$, $-1 \leq s \leq 10$.

Fig. (A) exhibits a traveling wave solution that characterizes the pulsatile blood flow in the forward direction. Before reaching to the bulge, blood flows in the form of traveling wave.

Fig. (B) exhibits three bright solitons with progressively decreasing solitary wave amplitude. Assuming homogeneous stratified layers of fluid, its flow is obtunded by presence of bulges. Depending upon the height of the bulge, a peculiar number of sheets of fluid curl upward to the peak of the bulge. The kinetic energy of each fluid sheet is partially converted into potential energy. Cumulative accretion of potential energy availed from each homogeneous sheet till the height of the bulge contributes to the creation of bright soliton at the apex of the bulge. The temporo-spatial localization of its energy and narrowing of time duration contributes to increment in wave speed. It can not be further emphasized that wave speed at the peak of the bulge is maximum. As the wave propagates further, its speed is progressively retarded because bright

soliton vanishes after the peak of the bulge. In our case, this slower wave comes in contact with another bulge of almost same height, again a bright soliton emerges through the same postulated mechanism. At last, we see a bright soliton of least height suggestive of minimum height of the bulge.

Fig.(C) and (D) exhibits a standing wave with multiple breathers. The persistent localized standing breathers are created on the windward side of the bulge. The undulating array of breathers with opposite phases can be regarded as a standing wave. It is further emphasize that there is no standing wave in blood flow. The assemblage of multi-breathers with opposite phases appears as a standing wave. The initial oscillatory dynamics of multi-breathers with undulating amplitude is suggestive of the most unstable interaction among solitons. Gradually, the wave loses coherence and chaotic regime prevails. From physiological perspective it corresponds to phase transition from laminar to turbulent flow. Note that such multi-breathers interactions are not perfectly elastic.

Fig.(E) shows topological defect with one-dimensional kink. The presence of atleast two discontinuous fibro-fatty plaques (commonly present as bulges) may not be completely discrete to each other because these fibro-fatty plaques with distinct spatial localization are connected by one-dimensional kink. In higher dimensions, multiple topological defects can be connected by higher-dimensional kinks. It means that intra-arterial micro- and macro-transport is done through kink solitons. From physiological perspective, cargo transport in neurons and seminal vesicles is postulated as transport through solitons. Note that the solitary wave for intra-vascular transport is kink soliton.

Fig. (F) depicts an interaction of standing wave with bright and dark solitons. A bright soliton emerges at the peak of the bulge. The beaming correspondence among solitons presents the phase transition line to interact with an array of multiple breathers which appear as a standing wave. This results into propagation of nonlinear wave *i.e.* partially standing and partially traveling wave with variation in amplitude. Under physiological conditions, such solutions are unstable due to oscillatory instabilities.

7. CONCLUSION AND FUTURE SCOPE

The generalised (3+1)-dimensional NLEE is helpful to understand not only the instabilities but also the impact of the bulge on haemodynamic flow in an elastic compliant artery. In the present work, we provide physical explanation about physiological principles underlying blood flow in an elastic compliant artery with nonaxisymmetric bulge. To depict the role of wave-wave interaction on haemodynamic flow, we analysed (3+1)-dimensional NLEE. To seek intriguing representative examples of soliton, we obtained the infinitesimal generators, commutator table of Lie algebra, symmetry groups for the (3+1)-dimensional NLEE. By using Lie group transformations method, similarity reduction is conducted to find invariant solutions for the (3+1)-dimensional NLEE. Following features have been observed.

- Cumulative accretion of potential energy contributes to the creation of bright soliton at the apex of the bulge.
- The wave speed is maximum at the peak of the bulge and progressively retarded with antegrade flow.
- The persistent localized standing breathers are created on the windward side of the bulge.
- There is no standing wave in blood flow, rather it is the assemblage of multi-breathers with opposite phases appears as a standing wave.
- The solitary wave for intra-vascular transport is a kink soliton.

Therefore, understanding intricate dynamics of soliton interaction is essential to evaluate impact of nonaxisymmetric bulge on blood flow.

7.1. Future Scope. Our findings suggest that flow instabilities exist in an elastic compliant artery. To assess relationship between constitutive features and physiological adaptive process, novel in-vitro experiments and computational simulations

may be designed.

Compliance with ethical standards

Conflict of interest The authors declare no conflict of interest.

REFERENCES

- [1] M. D. Silver, Late complications of prosthetic heart valves, *Archives of pathology & laboratory medicine*, **102** (1978), no. 6, 281–4.
- [2] H.G. Bogren and M. H. Buonocore, Blood flow measurements in the aorta and major arteries with MR velocity mapping, *Journal of Magnetic Resonance Imaging*, **4** (1994), no. 2, 119–30.
- [3] V. Jadaun et al., Impact of solitons on the progression of initial lesion in aortic dissection, *Int. J. Biomath.* **15** (2022), no. 3, Paper No. 2150096, 24 pp.
- [4] R. Ross, Atherosclerosis: an inflammatory disease, *New England journal of medicine*, 340 (1999), no. 2, 115–26.
- [5] P. F. Davies, Flow-mediated endothelial mechanotransduction, *Physiological reviews*, 75 (1995), no. 3, 519–60.
- [6] K. R. O'Brien, B. R. Cowan, M. Jain, et al., MRI phase contrast velocity and flow errors in turbulent stenotic jets, *Journal of Magnetic Resonance Imaging: An Official Journal of the International Society for Magnetic Resonance in Medicine*, **28** (2008), no. 1, 210–8.
- [7] N. Westerhof, N. Stergiopoulos and M. Noble, *Snapshots of Hemodynamics*, 2005.
- [8] B. Eckhardt, T. M. Schneider, B. Hof, et al., Turbulence transition in pipe flow, *Annu. Rev. Fluid Mech.*, **39** 2007, no. 39, 447–68.
- [9] K. Avila, D. Moxey, D. Barkley D, et al., The onset of turbulence in pipe flow, *Science*, **333** (2011), no. 6039, 192–6.
- [10] M. Avila, A. P. Willis and B. Hof, On the transient nature of localized pipe flow turbulence, *Journal of Fluid Mechanics*, **646**(2010), 127–36.
- [11] D. Barkley, B. Song, V. Mukund, G. Lemoult, M. Avila, B. Hof, The rise of fully turbulent flow, *Nature*, **526** (2015) no. 7574, 550.
- [12] C. Thomas, A. P. Bassom, P. J. Blennerhassett and C. Davies, The linear stability of oscillatory Poiseuille flow in channels and pipes, *Proceedings of the Royal Society A: Mathematical, Physical and Engineering Sciences*, **467** (2011), no. 2133, 2643–62.
- [13] R. M. Nerem and W. A. Seed, An in vivo study of aortic flow disturbances, *Cardiovascular research*, **6** (1972), no. 1, 1–4.
- [14] J. Peacock, T. Jones, C. Tock and R. Lutz, The onset of turbulence in physiological pulsatile flow in a straight tube, *Experiments in fluids*, **24** (1998) no. 1, 1–9.
- [15] J. C. Stettler and A. F. Hussain, On transition of the pulsatile pipe flow, *Journal of fluid mechanics*, **170** (1986), 169–97.
- [16] R. Trip, D. J. Kuik, J. Westerweel and C. Poelma, An experimental study of transitional pulsatile pipe flow, *Physics of fluids*, **24** (2012), no. 1, 014103.
- [17] T.J. Pedley, *Fluid Mechanics of Large Blood Vessels*, Cambridge University Press, Cambridge, 1980.
- [18] Y.C. Fung, *Biodynamics: Circulation*, Springer-Verlag, New York, 1981.
- [19] H. Demiray, Wave propagation through a viscous fluid contained in a prestressed thin elastic tube, *Internat. J. Engrg. Sci.* **30** (1992), no. 11, 1607–1620.
- [20] G. Rudinger, Shock waves in a mathematical model of aorta, *J. Appl. Mech.* **37** (1970), 34–37.
- [21] S.C. Ling and H.B. Atabek, A nonlinear analysis of pulsatile blood flow in arteries, *J. Fluid Mech.* **55** (1972), 492–511.
- [22] V. Jadaun and N. R. Singh, *Mathematical Modeling and Well-Posedness of Three-Dimensional Shell in Disorders of Human Vascular System In Nonlinear Systems-Theoretical Aspects and Recent Applications*, IntechOpen,(2020).
- [23] M. Anliker, R.L. Rockwell and E. Ogden, Nonlinear analysis of flow pulses and shock waves in arteries, *Z. Angew. Math. Phys.* **22** (1968), 217–246.
- [24] R.J. Tait and T.B. Moodie, Waves in nonlinear fluid filled tubes, *Wave Motion* **6** (1984), 197–203.
- [25] R.S. Johnson, A nonlinear equation incorporating damping and dispersion, *J. Fluid Mech.* **42** (1970), 49–60.
- [26] Y. Hashizume, Nonlinear pressure waves in a fluid-filled elastic tube, *J. Phys. Soc. Jpn.* **54** (1985), 3305–3312.
- [27] H. Demiray, Solitary waves in a prestressed elastic tube, *Bull. Math. Biol.* **58** (1996), 939–955.
- [28] H.A. Erbay, S. Erbay and S. Dost, Wave propagation in fluid-filled nonlinear viscoelastic tubes, *Acta Mech.* **95** (1992), 87–102.
- [29] V. Jadaun, Pulsatile blood flow in healthy aorta: An application of nonlinear evolution equation, *Int. J. Biomath.* **15** (2022), no. 7, Paper No. 2250047, 30 pp.
- [30] R. Hirota, *The Direct Method in Soliton Theory*, Cambridge University Press, Cambridge (2004).
- [31] V.B. Matveev, M.A. Salle, *Darboux Transformation and Solitons*, Springer, Berlin (1991).
- [32] V. Jadaun and N. R. Singh, Soliton solutions of generalized $(3 + 1)$ -dimensional Yu-Toda-Sasa-Fukuyama equation using Lie symmetry analysis, *Anal. Math. Phys.* **10** (2020), no. 4, Paper No. 42, 24 pp.
- [33] M. J. Ablowitz and P. A. Clarkson, *Solitons, nonlinear evolution equations and inverse scattering*, London Mathematical Society Lecture Note Series, 149, Cambridge University Press, Cambridge, 1991.
- [34] M. Wang, X. Li and J. Zhang, The $(\frac{G'}{G})$ -expansion method and travelling wave solutions of nonlinear evolution equations in mathematical physics, *Phys. Lett. A* **372** (2008), no. 4, 417–423.

- [35] C. Rogers and W. F. Shadwick, *Bäcklund transformations and their applications*, Mathematics in Science and Engineering, 161, Academic Press, Inc., New York, 1982.
- [36] G. W. Bluman and S. Kumei, *Symmetries and differential equations*, Applied Mathematical Sciences, 81, Springer-Verlag, New York, 1989.
- [37] P. J. Olver, *Applications of Lie groups to differential equations*, second edition, Graduate Texts in Mathematics, 107, Springer-Verlag, New York, 1993.
- [38] V. Jadaun, Phys. Scr. <https://doi.org/10.1088/1402-4896/ac0031>, (2021).

VISHAKHA JADAUN, MALLA REDDY UNIVERSITY, HYDERABAD-500100, INDIA.
Email address, * Corresponding author: vishakhasjadaun@gmail.com